Research Article

Shenling Baizhu Powder Ameliorates Diabetic2 Nephropathy via PI3K-Akt Pathway

Li Li, Shanshan Liu, Yu Zhang and Lisha Liu[*]

Department of Supply and Insurance Center, Central Hospital, Shandong First Medical University, China

Abstract

Diabetic Nephropathy (DN) is one of the serious complications of diabetes. This study is aimed at exploring the mechanisms of Shenling Baizhu Powder (SLBZP) on depressive DN based on network pharmacology analysis and molecular docking. The active components, potential target, and action mechanism of SLBZP against DN were analyzed by network pharmacology. Then, the results of network pharmacology were validated in molecular docking and *in vivo* experiments of STZ-induced DN mouse model. Body weight, fasting blood glucose, and others biochemical indexes as well as H&E staining were used to assess protective effect of SLBZP on DN. Using ELISA and qRT-PCR assay to examined the expression levels of inflammatory cytokines (IL-1β, IL-6, IL-8, and TNF-α) in serum or kidney tissue. Western blot was used to detect the expression of PI3K-Akt pathway related proteins. We obtained 183 active components and 143 potential targets of SLBZP against DN. Network pharmacology analysis showed PI3K-Akt pathway may play important role in DN's development. By molecular docking analysis, we obtained a total of 69 docking pairs. In verified experiments, SLBZP regulated the levels of body weight, fasting blood glucose, and others biochemical indexes in DN mice. Moreover, SLBZP obviously improved kidney damage and decreased the expression of IL-1β, IL-6, IL-8, and TNF-α. Furthermore, SLBZP significantly suppressed the activity of the PI3K-Akt pathway. Current study found that SLBZP could improve DN, which was probably attributed to inhibiting PI3K-Akt activation. This finding provided the new perspective for DN treatment.

Keywords: Shenling Baizhu powder; Diabetic nephropathy; Network pharmacology; PI3K-Akt pathway

Introduction

Diabetic nephropathy (DN) is a complex and severe diabetic microvascular complication, with an estimated prevalence of up to 50% and possibly more [1]. It has emerged as the primary reason for End Stage Renal Disease (ESRD) [2]. The pathogenesis of DN is complex, Genetics, insulin resistance, hyperglycemia, and autoimmune processes are some of the possible reasons [3,4]. The main manifestations of DN are abnormal renal hemodynamics, blood glucose metabolism disorders, increased blood lipids, chronic inflammation, and oxidative stress and so on. At present, the treatment of this disease mainly relies on regulating diet to control blood sugar and blood pressure, and DN is difficult to cure [5]. Traditional Chinese Medicine (TCM) can be used as an ideal choice for the treatment of diabetic nephropathy [6,7]. Shenling Baizhu Powder (SLBZP) has its origins in the Song Dynasty of China, specifically from the "Prescriptions of Taiping Heji Bureau" (1148 A.D.). It is consisting of Ginseng, Poria, *Atractylodes macrocephala*, White Lentil, Lotus Seed, Yam, *Amomi Fructus*, *Coicis Semen*, *Platycodonis Radix*, and Licorice [8]. Studies have reported that SLBZP have effect on many diseases, such as nonalcoholic fatty liver disease [9], Pi (Spleen)-deficiency-induced functional diarrhea [10] and so on. Moreover, Poria, *Atractylodes macrocephala* extracts, and Licorice extract such as licorice flavonoids could decrease the blood glucose by increasing the

secretion of insulin, promoting the proliferation of pancreatic B cells and suppress disorders of lipid metabolism, and may play a role in diabetes [11-14]. Furthermore, SLBZP or in combination with other drugs is used in the treatment of patients with diabetic nephropathy in clinical studies [15-17]. However, the action mechanism of SLBZP on DN remains unclear Network pharmacology is a promising method that combines systematic network analysis and pharmacology [18]. In this study, we explore the components and targets as well as action mechanism of SLBZP against DN using network pharmacological method. Then, the binding ability of key components and hub targets were verified by molecular docking. Finally, we constructed a DN mouse model to identify the effect of SLBZP on DN. Our research provides a new drug for the treatment of DN.

Materials and Methods

Gathering active ingredients and probable targets of SLBZP

All components of SLBZP were acquired from TCM Systems Pharmacology (TCMSP), TCM Integrated Database (TCMID), and Herbal Ingredients' Targets Database (HIT) [19-21]. All targets of related to the effective active components of SLBZP were identifying in the TCM-ID, TCMSP, HIT, and Search Tool for Interacting Chemicals (STITCH) [22] databases. The related targets of SLBZP were screened based on the compound-target correlation score, which should be greater than 400. The target information was standardized through NCBI database. The active components were screened under the conditions of Quantitative Estimate of Drug-Likeness (QED) [23] ≥ 0.2. Then, the active elements and possible targets underwent additional screening using a binomial statistical approach based on prior research [24,25].

Gathering DN-associated targets

Searching Online Mendelian Inheritance in Man (OMIM), DisGeNet and GeneCard databases [26-28] were used to search DN-related disease targets with the key word "diabetic nephropathy". The duplicate targets were merged and deleted.

*Correspondence: Lisha Liu, Department of Supply and Insurance Center, Central Hospital, Shandong First Medical University, No.105, Jiefang Road, Jinan, 250013, China, E-mail: liulisha0310@163.com

Key target selection and Protein-Protein Interaction (PPI) building

The key targets of SLBZP acting on DN were determined by Venny 2.1 and then uploaded to the STRING database for PPI analysis, with the species set as "*Homo sapiens*". The PPI networks were integrated, analyzed, and visualized using Cytoscape 3.8.0 software. Then, 10 targets with higher degree scores were selected by Cytohubba (Cytoscape plug-in) as hub targets, and hub targets network was constructed by Cytoscape 3.8.0 software.

Construction of Drug-Active Components-Targets (D-C-T) network

To exhibit the interaction between the SLBZP components and targets acting on DN, the active components and key targets were selected and subsequently imported into Cytoscape 3.8.0 software to build a H-C-T network.

GO and KEGG enrichment analysis

To better illustrate the function of these key targets, pathway enrichment analyzes by GO and KEGG were performed by DAVID. Pathways were ranked based on the number of molecules, and cutoff value was set as P<0.01 meaning for significant enrichment.

Molecular docking

Top 9 targets (AKT1, IL6, TP53, MAPK3, TNF, ALB, VEGFA, CXCL8, CCL2) and 8 components (isoliensinine, diosgenin, acacetin, liquiritin, higenamine, (20S)-protopanaxatriol, pachymic acid, scopoletin) were selected as core targets and core components for molecular docking. The chemical structural of the 8 active compounds contained in SLBZP were downloaded from the Zinc website [29]. Targets' 3D structures were obtained from PDB database [30]. PyMol 2.3.0 [31] was used to separate the target protein from the original ligand and remove the water molecule. Then, the ligand and receptor were imported into AutoDockTools 1.5.6 [32] for adding polar hydrogen and distributing charges. The file was saved in 'pdbqt' format. Finally, the molecular docking was carried out using AutoDock Vina 1.1.2 [33] and the binding energy (affinity) was analyzed by PyMol.

Mouse model and treatment

Male C57BL/6 J mice (8-week-old, 20 g to 25 g), purchased from GemPharmatech Co. Ltd. (Nanjing, China), were housed in a controlled room with alternate 12 h light/dark each day. All animal studies were approved by Ethics Committee of Xiamen University (XMULAC20220034-6). After one week, all mice were randomly allocated into 5 groups (6 mice per group): control, model, low-dose SLBZP, mid-dose SLBZP, and high-dose SLBZP groups. Except for the control group, 50 mg/kg of streptozotocin (STZ, Sigma-Aldrich, MO, USA) was intraperitoneally injected into each group daily for 5 days to establish DN mouse model. Mice with a glucose concentration of 11 mM-18 mM were a successful diabetic mouse model. The mice in the SLBZP groups were given SLBZP orally at 1 g/kg (low-dose), 2 g/kg (mid-dose), and 4 g/kg (high-dose) once daily for 5 weeks, respectively. The model group mice were given equal amounts of saline. Body weight and fasting blood glucose concentration of all mice were measured using a blood glucometer (One Touch Ultra, Lifescan, Johnson & Johnson Milpitas, CA, USA) weekly for 5 weeks. Then, at the end of administration, blood and urine samples were collected from all mice after 6 h fasting, serum total Cholesterol (TC), serum total Triglyceride (TG), Serum Creatinine (SCr), Blood Urea Nitrogen (BUN), 24 h albuminuria, and the Albumin-Creatinine

Ratio (ACR) was measured using a fully automated biochemical analyzer (Roche, China). In the end, the mice were anesthetized using sodium pentobarbital (i.p., 35 mg/kg) and euthanized through cervical dislocation. Kidney tissue was removed and weighed.

Hematoxylin and Eosin (H&E) staining

Kidney tissues were submerged in 4% paraformaldehyde, dehydrated through a series of ethanol concentrations (ascending), embedded in paraffin, and sectioned into 5 μm slices. The sections were deparaffinized with xylene and subsequently stained with hematoxylin for 3 min and eosin for 2 min. Images of H&E-stained samples were captured using a light microscope (Olympus, Japan).

ELISA assay

Inflammatory cytokine levels, including interleukin 6 (IL-6), interleukin 8 (IL-8), interleukin 1β (IL-1β), and tumor necrosis factor-α (TNF-α), were assessed in serum or kidney tissue samples using ELISA kits (Invitrogen, CA, USA) based on the manufacturer's illustration. The concentrations of cytokines were measured using microplate reader at 450 nm (DR-200Bs, Wuxi Hiwell Diatek, Wuxi, China).

Quantitative Real-time PCR (qRT-PCR)

Total RNA was isolated from the fresh kidney tissues using Trizol buffer (Invitrogen), and then converted into cDNA using PrimeScript™ RT reagent Kit (Takara, Japan). The qRT-PCR was conducted using SYBR green Master Mix (Bio-rad Laboratory, CA, USA) on the 7500 real-time PCR system (Applied Biosystems, CA, USA). The relative expression of target genes was examined with 2-ΔΔCT method and normalized to GAPDH. Primer sequences are listed in Table 1.

Western blot

Protein was extracted by RIPA lysis buffer (Beyotime, China) from fresh kidney tissues, separated by SDS-PAGE, and transferred to membrane. After sealed with 5% non-fat milk, the membranes were 135 incubated with p-PI3K (1:1000; CST, MA, USA, #4228), PI3K (1:1000; CST, #4257), p-Akt (1:1000; CST, #9271), Akt (1:1000; CST, #9272), p-P65 (1:1000; CST, #3033), P65 (1:1000; CST, #6956), and GAPDH antibodies (1:1000, Abcam, UK, ab245355) at 4°C overnight and followed by secondary antibodies (1:1000; Proteintech group, Wuhan, China, SA00001-1 (goat anti-mouse) or SA00001-2 (goat anti-rabbit)) for 1 h at 25°C. Then, Bands were exhibited using ECL Plus Detection System (Millipore, Germany).

Statistics analysis

Data were analyzed using GraphPad Prism v.9 software and presented as mean ± standard deviation. Group comparisons were performed utilizing one-way or two-way analysis of variance. Statistical significance was determined by a P-value of less than 0.05.

Results

Active components and potential targets of SLBZP

A total of 337 active components and 8,227 potential targets of SLBZP were harvested from public databases. After been screened by QED ≥ 0.2, we obtained 289 active components of SLBZP. And followed by binomial statistical model analysis, 811 potential targets and 243 active compounds of SLBZP were obtained.

Targets of DN

The DN-related targets were obtained from three databases: OMIM, DisGeNet, and GeneCard and 108, 405 and 378 targets were

Table 1: Common targets of SLBZP and DN.

ID	Name	ID	Name	ID	Name	ID	Name
19	ABCA1	1268	CNR1	3479	IGF1	5444	PON1
32	ACACB	1277	COL1A1	3480	IGF1R	5465	PPARA
1636	ACE	1376	CPT2	3586	IL10	5468	PPARG
60	ACTB	1385	CREB1	3552	IL1A	10891	PPARGC1A
9370	ADIPOQ	1499	CTNNB1	3553	IL1B	5578	PRKCA
134	ADORA1	3627	CXCL10	3558	IL2	5579	PRKCB
154	ADRB2	58191	CXCL16	3569	IL6	5728	PTEN
155	ADRB3	3576	CXCL8	3630	INS	5743	PTGS2
183	AGT	1644	DDC	3643	INSR	5970	RELA
185	AGTR1	1666	DECR1	3667	IRS1	5972	REN
186	AGTR2	1906	EDN1	3687	ITGAX	6010	RHO
7965	AIMP2	1909	EDNRA	3827	KNG1	5054	SERPINE1
231	AKR1B1	1956	EGFR	3952	LEP	23411	SIRT1
207	AKT1	1958	EGR1	3958	LGALS3	6514	SLC2A2
213	ALB	2033	EP300	4023	LPL	6517	SLC2A4
51129	ANGPTL4	2099	ESR1	4036	LRP2	6647	SOD1
335	APOA1	2149	F2R	5594	MAPK1	6648	SOD2
338	APOB	2150	F2RL1	1432	MAPK14	6720	SREBF1
348	APOE	2168	FABP1	5595	MAPK3	6750	SST
506	ATP5F1B	2167	FABP4	5599	MAPK8	6774	STAT3
567	B2M	2335	FN1	4313	MMP2	7018	TF
596	BCL2	2571	GAD1	4318	MMP9	7057	THBS1
627	BDNF	2572	GAD2	4353	MPO	7097	TLR2
718	C3	2641	GCG	2475	MTOR	7099	TLR4
727	C5	2678	GGT1	4843	NOS2	7124	TNF
836	CASP3	156	GRK2	4846	NOS3	7157	TP53
841	CASP8	2932	GSK3B	50507	NOX4	7173	TPO
842	CASP9	2936	GSR	4852	NPY	7200	TRH
847	CAT	3091	HIF1A	1728	NQO1	57761	TRIB3
6347	CCL2	3105	HLA-A	8856	NR1I2	7276	TTR
1490	CCN2	3106	HLA-B	142	PARP1	7351	UCP2
729230	CCR2	3162	HMOX1	3651	PDX1	10911	UTS2
1234	CCR5	3240	HP	5290	PIK3CA	2837	UTS2R
948	CD36	3339	HSPG2	5328	PLAU	7412	VCAM1
920	CD4	3356	HTR2A	5340	PLG	7422	VEGFA
55748	CNDP2	3383	ICAM1	5443	POMC		

found respectively. Among them, 709 targets were finally obtained after removed duplicate targets.
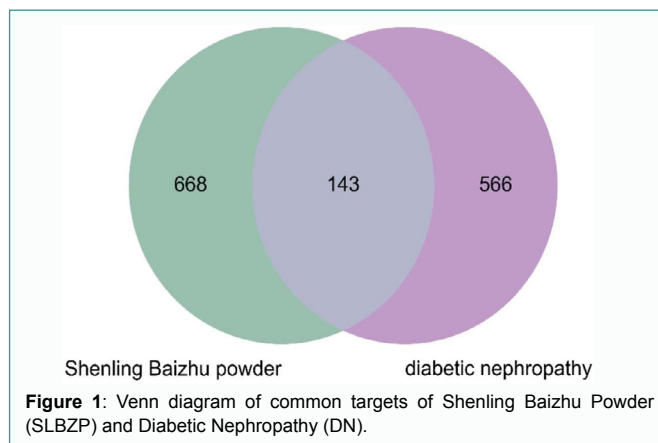
Key target screening and PPI construction

The predictive targets of active components of SLBZP were intersected with DN-related targets, 143 overlapping targets were obtained and Venn maps were drawn as Figure 1. Detailed information of the common target is shown in Table 1. The common targets were submitted to the STRING database to build PPI network, as shown in Figure 2. A total of 143 nodes and 3382 edges were contained in the network and the average degree was 48.7. The nodes with the top five degrees were INS, ALB, AKT1, IL6, and TNF. These targets were likely to play a critical role in DN progress. Additionally, we have obtained 183 active compounds of SLBZP according to these 143 common targets.

Construction of D-C-T network

The D-C-T network was constituted with 102 active components and 214 targets, as shown in Figure 3. The results showed that 10 active components of SLBZP such as palmitic acid, IFP, quercetin, adenosine, CLR, choline, oleic acid, dopamine, LDP and L-Lysin have a high degree of connectivity and mediation with DN targets. Palmitic acid had the maximum number of potential targets with 94, followed by IFP with 69 potential targets.

GO and KEGG pathway enrichment analysis

The 143 common targets were run by R-package. A total of 1649

Figure 1: Venn diagram of common targets of Shenling Baizhu Powder (SLBZP) and Diabetic Nephropathy (DN).

GO terms were obtained, which including 1537 of Biological Process (BP), 46 of Cellular Component (CC), and 66 of Molecular Function (MF) (P<0.01). Top 15 functional information sets were selected for analysis and mapping (Figure 4A-C). The main BP involved in the common targets were related to reactive oxygen species metabolic process, response to nutrient levels, response to molecule of bacterial origin, multicellular organismal homeostasis, response to lipopolysaccharide, etc. In addition, main terms of CC were associated with vesicle lumen, cytoplasmic membrane-bounded vesicle lumen, membrane raft, membrane microdomain, secretory granule lumen, etc. MF enrichment was mainly involved in receptor agonist activity,
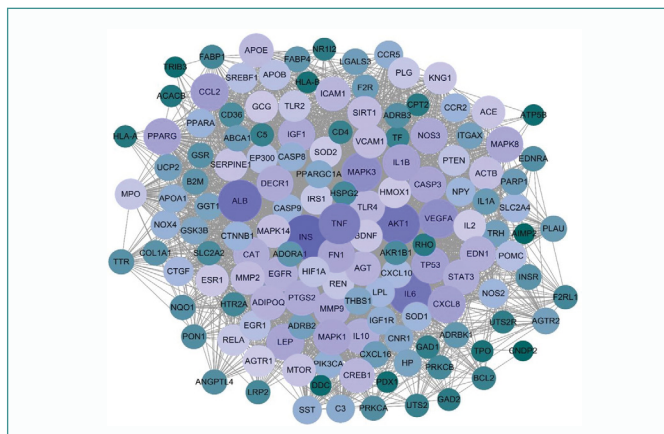
Figure 2: Protein-protein interaction (PPI) network of common targets.
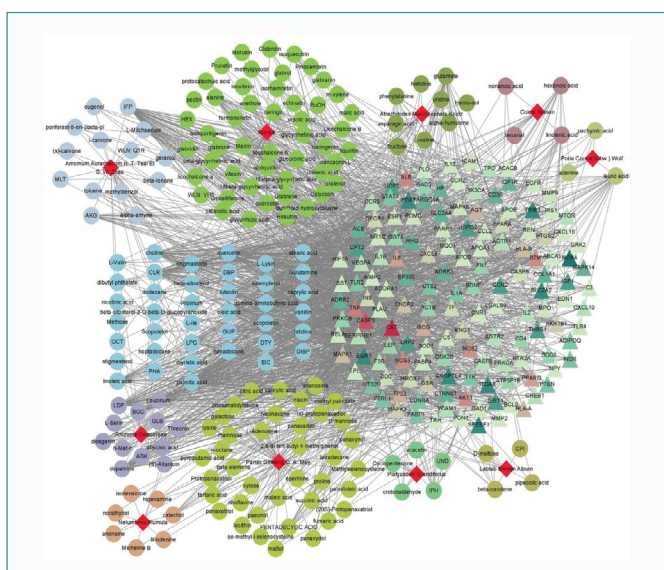

Figure 3: Drug-active components-targets (D-C-T) network. The triangle is the key targets of SLBZP against DN, the circles represent compounds, different colors represent compounds contained in different herbs, where the light green circles represent compounds contained in a variety of herbs, the red quadrilateral represents different herbs.
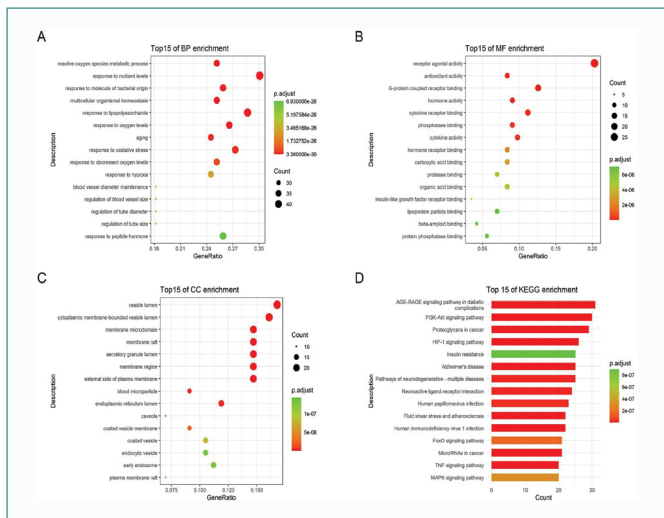

Figure 4: The top 15 terms of GO and KEGG enrichment analysis. (A) Biological process (BP); (B) Molecular function (MF); (C) Cellular component (CC); (D) KEGG pathway.

antioxidant activity; G-protein coupled receptor binding, hormone activity, cytokine receptor binding, etc. These processes may play a vital role in the development of DN.

KEGG enrichment analysis yielded a total of 161 pathways. Similarly, the top 15 KEGG pathways were selected and showed in Figure 4D according P value less than 0.01. It included the AGE-RAGE signaling pathway in diabetic complications, PI3K-Akt signaling pathway, Proteoglycans in cancer, HIF-1 signaling pathway, Insulin resistance, etc.

Construction of target-BP-pathway network

The network of target-BP-pathway was constructed by Cytoscape and showed in Figure 5. There are 159 nodes and 1736 edges in the network. Among these nodes belonging to three categories, AKT1, response to nutrient levels, AGE-RAGE signaling pathway in diabetic complications had the most edges with 29, 43, 31, respectively. To analyze the correlation of core targets with BP and pathways more clearly and intuitively, core targets network including 10 targets was constructed by String database and Cytoscape (Figure 6A). Then the correlations were visualized (Figure 6B and C). Among the 10 core targets, AKT1 is pivotal with the greatest connectivity with BP and pathways. It is predicted that AKT1 is an important target in the intervention of DN.
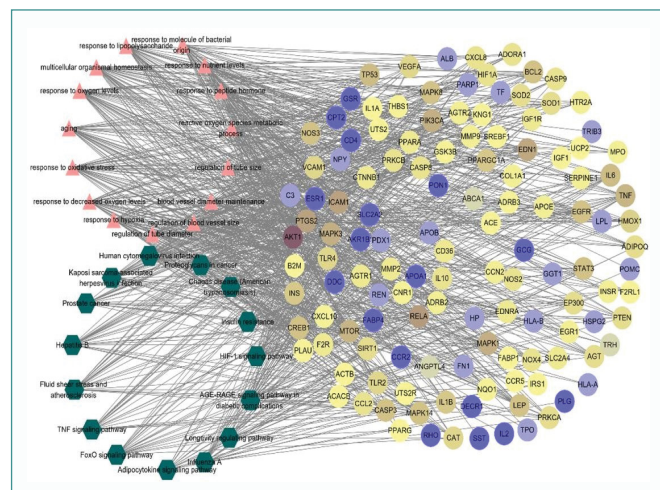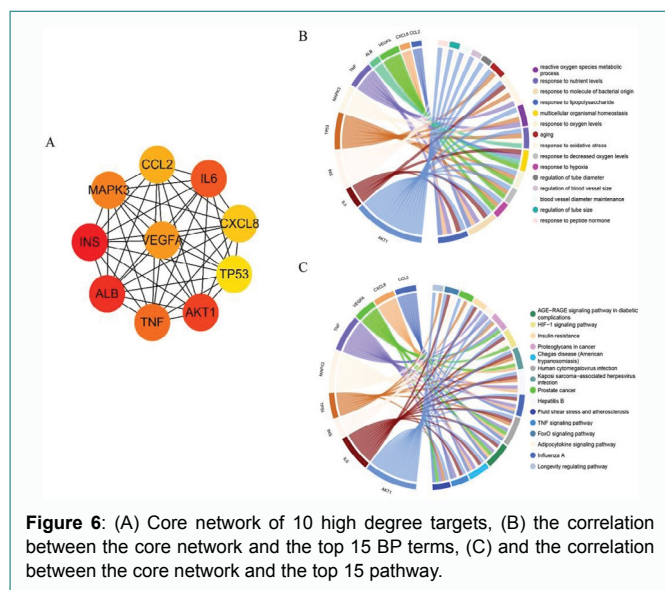

Figure 5: Target-BP-pathway network. The circles represent core targets, triangles represent biological processes and hexagons represent signal pathways.

Molecular docking results

Molecular docking was applied to validate the binding action mode of 8 compounds with 9 core targets, according to the network analysis. The structure diagrams of 8 compounds were shown in Table 2. A total of 69 pairs of docking were obtained and showed in Table 3. The results showed that the affinities were all less than 5 kcal/mol, indicating that they had strong binding activity. The smaller the value, the easier the active ingredient binds to the targets. The top 10 binding modes of the core targets and their corresponding compounds were showed in Figure 7. The affinity of isoliensinine with the targets such as ALB, AKT1 and MAPK3, diosgenin with AKT1, acacetin and liquiritin with ALB were all less than 10 kcal/mol, indicated that these active ingredients had strong binding activity with the corresponding targets.

SLBZP improved renal function and kidney damage

Figure 6: (A) Core network of 10 high degree targets, (B) the correlation between the core network and the top 15 BP terms, (C) and the correlation between the core network and the top 15 pathway.

To verify the effect of SLBZP on DN, we constructed a STZ-induced DN mouse model. Diabetes mellitus' biomarker is the level of fasting blood glucose. Compared with the control group, the other groups showed significantly higher fasting blood glucose levels on week 0, suggesting that STZ was effective in inducing diabetes in mice. Then, SLBZP dose-dependently treatment decreased fasting blood glucose level in STZ-induced diabetic mice over the following weeks (Figure 8A). Moreover, as seen in Figure 8 B, mice in control group displayed a continuous increased in body weight, in contrast, mice in model group were inhibited this growth. Meanwhile, SLBZP administer significantly reversed the inhibitory effect of STZ on weight gain.

To assess the protective effect of SLBZP on DN, we measured biochemical indicators levels of renal function, including the ratio of kidney weight to body weight, SCr, BUN, TC, TG, ACR, and 24 h albuminuria. Compared with the control group, these biochemical indicators levels were significantly increased in model group. Addition of SLBZP could dose-dependently attenuated these biochemical indicators levels in STZ-induced diabetic mice (Figure 8 C-I). Additionally, we assessed the protective effect of SLBZP on DN at the pathological level. H&E staining outcomes indicated significant kidney tissue damage in the model group, such as enlarged glomeruli, thickened glomerular basement membrane, vacuolated tubular degeneration, and infiltrating inflammatory cells. Following SLBZP treatment, there was a reduction in glomerular volume, improvement in glomerular basement membrane thickening, decreased tubular vacuolation, and diminished inflammatory cell infiltration to different extents in all cases (Figure 8 J).

SLBZP weakened the inflammatory response

To determine the inhibitory role of SLBZP on inflammation in DN mice, we detected the expression of inflammatory cytokines, including IL-1β, IL-6, IL-8, and TNF-α in the serum or kidney tissues. Compared with the control group, STZ-injection remarkably increased the expression of IL-1β, IL-6, IL-8, and TNF-α in the serum of DN mice. Additionally, administration of SLBZP was significantly weakened the enhancement induced by STZ (Figure 9A). Moreover, the protein (Figure 9B) and mRNA (Figure 9C) expression of these inflammatory cytokines in the kidney tissues exhibited a similar patten as in the serum.

SLBZP suppressed the PI3K-AKT pathway

To explore the action mechanism of SLBZP against DN, we examined the expression of PI3K-Akt pathway-related proteins using western blot based on network pharmacological analysis. STZ-injection obviously elevated the expression of p-PI3K, p-Akt, p-P65, and P65 in the kidney tissue of DN mice, which can be significantly attenuated by SLBZP dose-dependent addition. Additionally, PI3K and Akt expression had no changed in all groups (Figure 10).
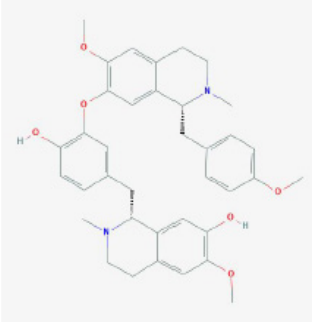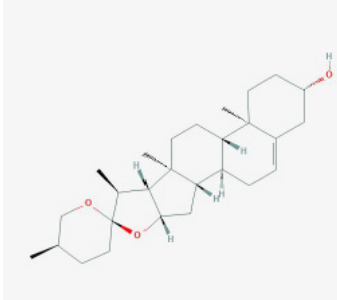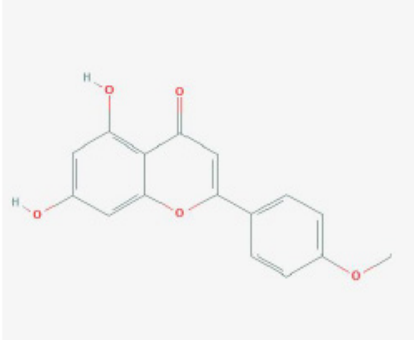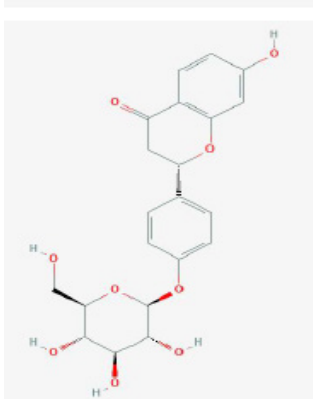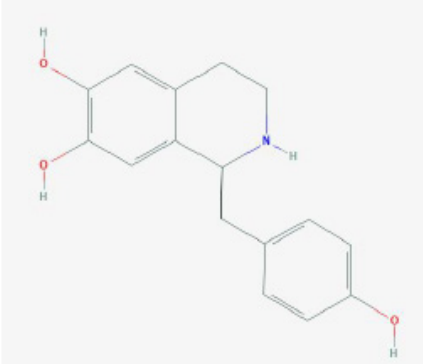
Discussion

DN is a serious complication of diabetes. Disorders of glucose and lipid metabolism, inflammatory response stimulation, and oxidative stress can cause a decrease in renal metabolic function. At present, the treatment of DN has not made breakthrough progress. SLBZP contains a variety of active ingredients, which have the beneficial effect on endocrine and metabolic disorders in DN development.

In the present study, 183 active ingredients of SLBZP and 143 DN-related targets were screened out through network pharmacology analysis. It indicates that SLBZP influences DN, which is achieved through the combined action of multiple components and multiple targets. The D-C-T network showed that the active compounds, including quercetin, adenosine, and dopamine have a high degree of connectivity and mediation with DN targets, suggesting that they may play an important role in the treatment of DN by SLBZP. Quercetin, being the flavonoids compounds exists in plants widely, which has many biological activities such as anti-oxidation, anti-inflammatory, lowering blood sugar, and lowering blood lipids, and has broad pharmacological value. Quercetin can affect glucose and lipid

Metabolism disorders in the body through various pathways such as Akt, SIRT1, PI3K/AKT, and endoplasmic reticulum stress [34,35]. Adenosine is an endogenous purine nucleoside molecule which can be induced when cell damage or inflammation occurs. Adenosine can act as an insulin regulator by controlling insulin signals in adipose tissue, muscle, and liver, and indirectly affect inflammation and immune cells in these tissues [36]. Dopamine is a key neurotransmitter in the hypothalamus and pituitary gland; it has the effect of stimulating adrenergic α and β receptors. It can dilate renal blood vessels and increase renal blood flow and glomerular filtration rate [37]. The PPI network of 143 common targets showed that SLBZP against DN may be relied on INS, ALB, AKT1, IL6, TNF, etc. core targets. INS, ALB, AKT1, IL6, and TNF participate in the BP of inflammatory response, oxidative stress, and lipid metabolic process and can be involved in the development and progression of DN through various pathways [38]. Moreover, IL-6 is a biomarker of chronic kidney injury, which mediates inflammatory response through gp130-STAT3-dependent mechanism, and essential for the progression of DN2017 [39,40]. The KEGG pathway analysis proved that SLBZP exerted on DN through various signaling pathway, including AGE-RAGE, PI3K-Akt, and HIF-1 pathways. The AGE-RAGE signaling pathway in diabetic complications is the most critical signaling pathway in DN. It can not only activate NF-κB and NADPH oxidase to cause oxidative stress reactive oxygen species, but also stimulate the production of VEGF and enhance the expression of TGF-β1 [3]. Moreover, as an upstream mediator of NF-κB, PI3K-Akt signaling pathway has been shown to play an important role in the proliferation, cell cycle progression and cell viability of DN [41]. Hu et al. [42] found that inhibition of PI3K-AKT activation reduced urinary protein excretion and improved renal injury in DN rats, further improving DN. In addition, Jin et al. [43,44] showed that inhibition of PI3K-AKT activation enhanced podocyte

Table 2: The structure diagrams of 8 compounds.

Synonyms	Molecular Formula	2D Structure
isoliensinine	C27H42O3	
diosgenin	C30H52O4	
acacetin	C10H8O4	
Liquiritin	C16H12O5	
higenamine	C37H42N2O6	
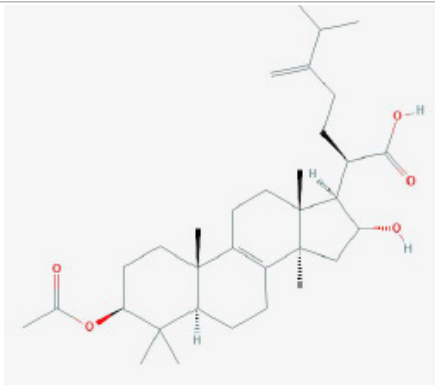
(20S)-Protopanaxatriol	C16H17NO3	
pachymic acid	C15H18O2	

Table 3: The results of molecular docking.

| Chemical	PDB	GENE	Best affinity
isoliensinine	1n5u	ALB	-13.1
isoliensinine	6buu	AKT1	-10.8
isoliensinine	4qtb	MAPK3	-10.7
diosgenin	6buu	AKT1	-10.4
acacetin	1n5u	ALB	-10.1
Liquiritin	1n5u	ALB	-10.1
Liquiritin	4qtb	MAPK3	-10
isoliensinine	2nz1	CCL2	-9.8
higenamine	1n5u	ALB	-9.8
Liquiritin	2e7a	TNF	-9.6
Liquiritin	2nz1	CCL2	-9.6
diosgenin	2e7a	TNF	-9.5
isoliensinine	2e7a	TNF	-9.5
(20S)-Protopanaxatriol	6buu	AKT1	-9.4
diosgenin	2nz1	CCL2	-9.2
(20S)-Protopanaxatriol	2nz1	CCL2	-9.2
Liquiritin	1xqh	TP53	-9.2
isoliensinine	1xqh	TP53	-9
Liquiritin	6buu	AKT1	-9
(20S)-Protopanaxatriol	1xqh	TP53	-8.9
(20S)-Protopanaxatriol	2e7a	TNF	-8.9
pachymic acid	6buu	AKT1	-8.9
pachymic acid	2nz1	CCL2	-8.7
acacetin	4qtb	MAPK3	-8.6
higenamine	6buu	AKT1	-8.6
acacetin	2e7a	TNF	-8.5
higenamine	2e7a	TNF	-8.5
higenamine	4qtb	MAPK3	-8.4
(20S)-Protopanaxatriol	1flt	VEGFA	-8.3
acacetin	1xqh	TP53	-8.3
acacetin	6buu	AKT1	-8.2
higenamine	1xqh	TP53	-8.2
Liquiritin	4j4l	IL6	-8.2
diosgenin	4qtb	MAPK3	-8
acacetin	2nz1	CCL2	-8
higenamine	2nz1	CCL2	-8
diosgenin	1xqh	TP53	-7.9
(20S)-Protopanaxatriol	1n5u	ALB	-7.9
scopoletin	1n5u	ALB	-7.8
isoliensinine	1flt	VEGFA	-7.6
scopoletin	1xqh	TP53	-7.5
acacetin	4j4l	IL6	-7.5
Liquiritin	1flt	VEGFA	-7.4
acacetin	1flt	VEGFA	-7.3
isoliensinine	4j4l	IL6	-7.3
higenamine	1flt	VEGFA	-7.3
pachymic acid	4qtb	MAPK3	-7.3
diosgenin	4j4l	IL6	-6.9
scopoletin	4qtb	MAPK3	-6.9
higenamine	4j4l	IL6	-6.9
(20S)-Protopanaxatriol	4qtb	MAPK3	-6.7
scopoletin	2e7a	TNF	-6.6
pachymic acid	2e7a	TNF	-6.6
diosgenin	6wzm	CXCL8	-6.5
scopoletin	6buu	AKT1	-6.5
higenamine	6wzm	CXCL8	-6.4
scopoletin	2nz1	CCL2	-6.3
(20S)-Protopanaxatriol	4j4l	IL6	-6.2
pachymic acid	1xqh	TP53	-6.2
(20S)-Protopanaxatriol	6wzm	CXCL8	-6.1
pachymic acid	1n5u	ALB	-6.1
diosgenin	1flt	VEGFA	-6
scopoletin	4j4l	IL6	-5.9
scopoletin	1flt	VEGFA	-5.8
pachymic acid	4j4l	IL6	-5.7
pachymic acid	1flt	VEGFA	-5.7
acacetin	6wzm	CXCL8	-5.4
scopoletin	6wzm	CXCL8	-5.1
pachymic acid	6wzm	CXCL8	-5.1

autophagy and reduced renal injury in DN rats. HIF-1 is a cytokine and exists widely in human body under hypoxic environment. It can regulate the expression of downstream cytokine VEGF, promote the formation of new blood vessels, relieve renal hypoxia and then slow down the progression of the disease.

Figure 7: Molecular docking diagram of core genes and core compounds. (A) Isoliensinine interacted action mode with ALB; (B) Isoliensinine interacted action mode with AKT1; (C) Isoliensinine interacted action mode with MAPK3; (D) Diosgenin interacted action mode with AKT1; (E) Acacetin interacted action mode with ALB; (F) Liquiritin interacted action mode with ALB; (G) Liquiritin interacted action mode with MAPK3; (H) Isoliensinine interacted action mode with CCL2; (I) Higenamine interacted action mode with ALB; (J) Liquiritin interacted action mode with TNF.

Figure 8: SLBZP improved renal function and kidney damage in DN mice. (A) Fasting blood glucose; (B) Body weight; (C) The ratio of kidney weight to body weight; (D) Serum Creatinine (SCr); (E) Blood Urea Nitrogen (BUN); (F) serum Total Cholesterol (TC); (G) serum total Triglyceride (TG); (H) the Albumin-Creatinine Ratio (ACR); (I) 24 h albuminuria. (J) Hematoxylin and Eosin (H&E) staining were used to evaluation the kidney damage, scale bar: 40 x. ***$P<0.001$ compared to control group; #$P<0.05$, ##$P<0.01$, and ###$P<0.001$ compared to model group; δ$P<0.05$, δδ$P<0.01$, and δδδ$P<0.001$ compared to low-dose SLBZP group.

In this study, the molecular docking results revealed that the compounds of SLBZP bind well to the potential targets for the treatment of DN. Additionally; we established a STZ-induced DN mouse model. *In vivo* experiments demonstrated that SLBZP could improve the renal damage and regulated the biochemical indexes levels. In addition, the results of *in vivo* experiments in mice also suggested that SLBZP could suppress the inflammatory response of the body - reducing the expression of inflammatory factors. Furthermore, the western blot results indicated that SLBZP alleviated DN symptoms probably through the PI3K-Akt signaling pathway.

Conclusions

In this study, we obtained 183 active components and 143 potential targets of SLBZP against DN. Key components have strong binding activity with their targets. *In vivo* experiments, SLBZP obviously improved kidney damage and decreased the expression of IL-1β, IL-6, IL-8, and TNF-α [45]. Moreover, SLBZP ameliorated DN may through PI3K-Akt signaling pathway. We expect these results will be useful and provide theoretical basis for subsequent clinical research for DN. However, there is a lack of clinical data to support this study, which will be the focus of our future study.
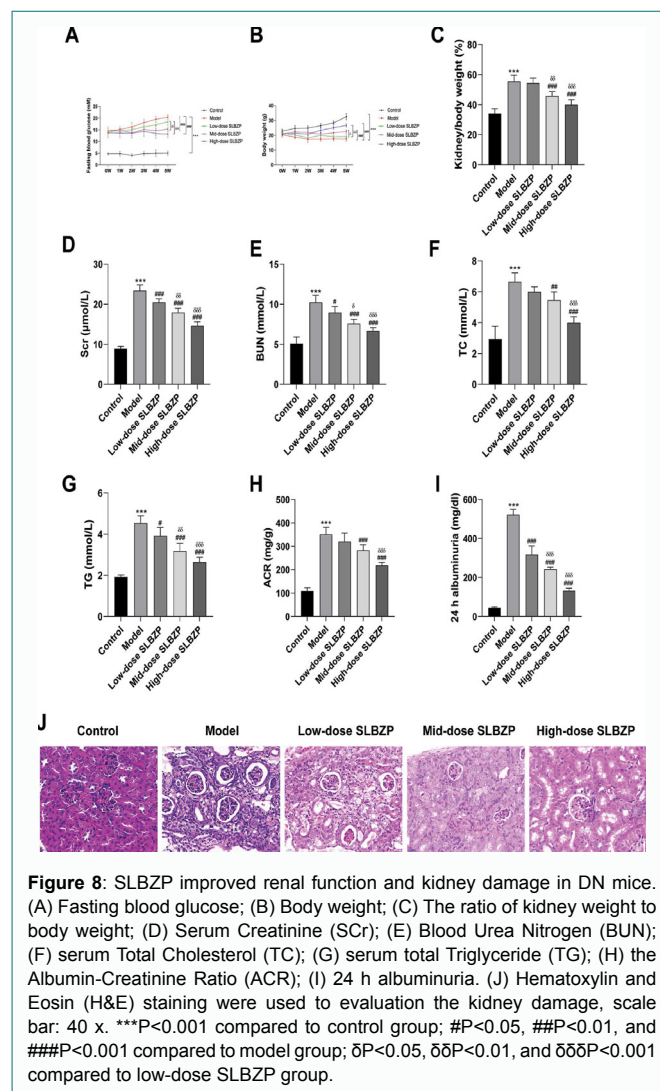
Ethical Approval

This study was approved by the Ethic Committee of XIAMEN UNIVERSITY (XMULAC20220034-6).

Conflicts of Interest

The authors declare that they have no conflicts of interest to report regarding the present study.

References

1. Yorek M. Treatment for diabetic peripheral neuropathy: What have we learned from animal models? Curr Diabetes Rev. 2022;18(5):e040521193121.

2. Liang S, Cai GY, Chen XM. Clinical and pathological factors associated with progression of diabetic nephropathy. Nephrology (Carlton). 2017;22 Suppl 4:14-9.

3. Lal MA, Patrakka J. Understanding podocyte biology to develop novel kidney therapeutics. Front Endocrinol (Lausanne). 2018;9:409.

4. Yang J, Li L, Hong S, Zhou Z, Fan W. LINK-A lncRNA activates HIF1 α signaling and inhibits podocyte cell apoptosis in diabetic nephropathy. Exp Ther Med. 2019;18(1):119-24.

5. Fu H, Liu S, Bastacky SI, Wang X, Tian XJ, Zhou D. Diabetic kidney diseases revisited: A new perspective for a new era. Mol Metab. 2019;30:250-63.

6. Wen Y, Yan M, Zhang B, Li P. Chinese medicine for diabetic kidney disease in China. Nephrology (Carlton). 2017;22 Suppl 4:50-5.

7. Zhang L, Yang L, Shergis J, Zhang L, Zhang AL, Guo X, et al. Chinese herbal medicine
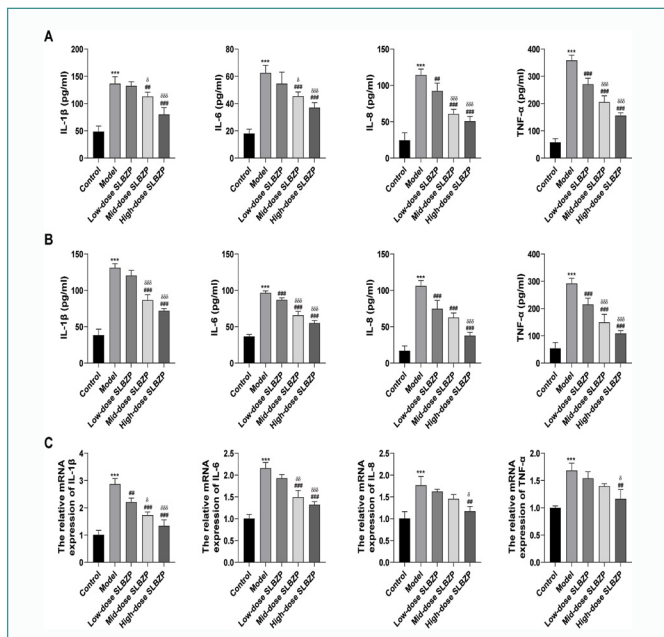
Figure 9: Effects of SLBZP treatment on renal inflammatory responses in DN mice. The expression levels of interleukin 6 (IL-6), interleukin 8 (IL-8), interleukin 1β (IL-1β), and tumor necrosis factor-α (TNF-α) in the serum (A) or kidney tissues (B) were measured using ELISA assay. (C) The relative mRNA expression levels of IL-6, IL-8, IL-1β, and TNF-α in the renal tissues were tested by qRT-PCR. ***P<0.001 compared to control group; ##P<0.01 and ###P<0.001 compared to model group; δP<0.05, δδP<0.01, and δδδP<0.001 compared to low-dose SLBZP group.

for diabetic kidney disease: a systematic review and meta-analysis of randomised placebo-controlled trials. BMJ Open. 2019;9(4):e025653.

8. Meng M, Bai C, Wan B, Zhao L, Li Z, Li D, et al. A Network Pharmacology-Based Study on Irritable Bowel Syndrome Prevention and Treatment Utilizing Shenling Baizhu Powder. Biomed Res Int. 2021;2021:4579850.

9. Pan MX, Zheng CY, Deng YJ, Tang KR, Nie H, Xie JQ, et al. Hepatic protective effects of Shenling Baizhu powder, a herbal compound, against inflammatory damage via TLR4/NLRP3 signalling pathway in rats with nonalcoholic fatty liver disease. J Integr Med. 2021;19(5):428-38.

10. Xiao Y, Zhang K, Zhu SY, Deng XL, Chen XY, Fu NL, et al. Shenling Baizhu Powder

11. () Ameliorates Pi (Spleen)-Deficiency-Induced Functional Diarrhea in Rats. Chin J Integr Med. 2021;27(3):206-11.

11. Guo Y, Xin N, Dai RJ. Research progress on the mechanism of natural flavonoids in treatment of type 2 diabetes mellitus. Nat Prod Res Develop. 2017;29(10):1805-11.

12. Li TH, Hou CC, Chang CL, Yang WC. Anti-Hyperglycemic Properties of Crude Extract and Triterpenes from Poria cocos. Evid Based Complement Alternat Med. 2011;2011:128402.

13. Zhang WY, Zhang HH, Yu CH, Fang J, Ying HZ. Ethanol extract of Atractylodis macrocephalae Rhizoma ameliorates insulin resistance and gut microbiota in type 2 diabetic db/db mice. J Funct Foods 2017;39:139-51.

14. Zhao HY, Wang Y, Yong-Ping MA, Wang Y. Suppressive effect of licorice flavonoids on hyperglycemia and hyperlipidemia in type 2 diabetic rats. China J Mod Med. 2010.

15. Ge S, Yu X, Zhou D, Zhang H, Peng J. The level changing of serum MCP-1, IL-6, TNF-αfrom type 2 diabetic nephropathy patients administered with metformin and Shen Qin Baizhu powder. J Gansu Sci. 2019;31(1):73-6,118.

16. Lu Y. Evaluation of the efficacy of Jiawei Shenling Baizhu powder in the treatment of early diabetic nephropathy with spleen and kidney qi deficiency and stasis. Guangming traditional Chinese Medicine. 2017;32:1071-3.

17. Zhang H. Effectiveness of Jiawei Shenling Baizhu powder in the treatment of patients with early diabetic nephropathy with spleen-kidney qi deficiency and blood stasis. Contemporary Medicine Forum. 2016;14:167-168.

18. Kibble M, Saarinen N, Tang J, Wennerberg K, Mäkelä S, Aittokallio T. Network pharmacology applications to map the unexplored target space and therapeutic potential of natural products. Nat Prod Rep. 2015;32(8):1249-66.

19. Liu F, Fu Y, Wei C, Chen Y, Ma S, Xu W. The expression of GPR109A, NF-kB and IL-1 β in peripheral blood leukocytes from patients with type 2 diabetes. Ann Clin Lab Sci. 2014;44(4):443-8.

20. Ru J, Li P, Wang J, Zhou W, Li B, Huang C, et al. TCMSP: a database of systems pharmacology for drug discovery from herbal medicines. J Cheminform. 2014;6:13.

21. Ye H, Ye L, Kang H, Zhang D, Tao L, Tang K, et al. HIT: linking herbal active ingredients to targets. Nucleic Acids Res. 2011;39(Database issue):D1055-9.

22. Szklarczyk D, Santos A, von Mering C, Jensen LJ, Bork P, Kuhn M. STITCH 5: augmenting protein-chemical interaction networks with tissue and affinity data. Nucleic Acids Res. 2016;44(D1):D380-4.

23. Bickerton GR, Paolini GV, Besnard J, Muresan S, Hopkins AL. Quantifying the chemical beauty of drugs. Nat Chem. 2012;4(2):90-8.

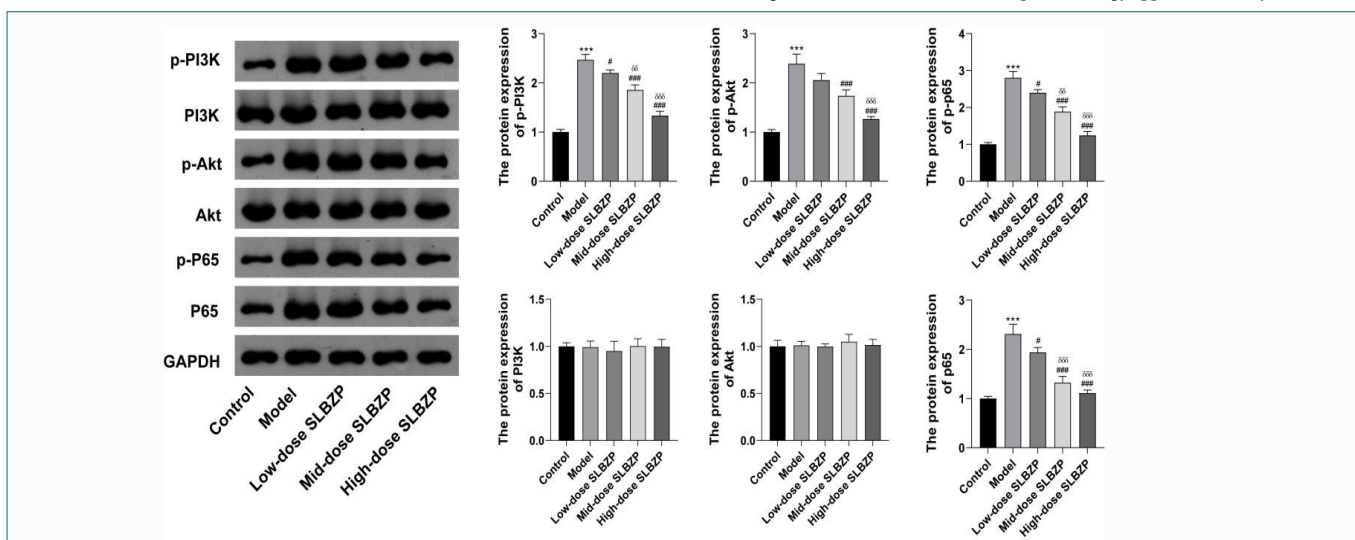24. Liang X, Li H, Li S. A novel network pharmacology approach to analyse traditional

Figure 10: SLBZP inhibited PI3K-Akt pathway in DN mice. Western blot was used to detect the protein levels of p-PI3K, PI3K, p-Akt, Akt, p-p65, and p65 in the renal tissues. ***P<0.001 compared to control group; #P<0.05, ##P<0.01, and ###P<0.001 compared to model group; δδP<0.01 and δδδP<0.001 compared to low-dose SLBZP group.

herbal formulae: the Liu-Wei-Di-Huang pill as a case study. Mol Biosyst. 2014;10(5):1014-22.

25. Yang M, Chen J, Xu L, Shi X, Zhou X, An R, Wang X. A network pharmacology approach to uncover the molecular mechanisms of herbal formula Ban-Xia-Xie-Xin-Tang. Evid Based Complement Alternat Med. 2018;2018:4050714.

26. Amberger JS, Hamosh A. Searching Online Mendelian Inheritance in Man (Omim): a knowledgebase of human genes and genetic phenotypes. Curr Protoc Bioinformatics. 2017;58:1.2.1-1.2.12.

27. Piñero J, Bravo À, Queralt-Rosinach N, Gutiérrez-Sacristán A, Deu-Pons J, Centeno E, et al. DisGeNET: a comprehensive platform integrating information on human disease-associated genes and variants. Nucleic Acids Res. 2017;45(D1):D833-9.

28. Safran M, Dalah I, Alexander J, Rosen N, Iny Stein T, Shmoish M, et al. GeneCards Version 3: the human gene integrator. Database (Oxford). 2010;2010:baq020.

29. Sterling T, Irwin JJ. ZINC 15--Ligand Discovery for Everyone. J Chem Inf Model. 2015;55(11):2324-37.

30. Burley SK, Berman HM, Kleywegt GJ, Markley JL, Nakamura H, Velankar S. Protein Data Bank (PDB): the single global macromolecular structure archive. Methods Mol Biol. 2017;1607:627-41.

31. Seeliger D, de Groot BL. Ligand docking and binding site analysis with PyMOL and Autodock/Vina. J Comput Aided Mol Des. 2010;24(5):417-22.

32. Morris GM, Huey R, Lindstrom W, Sanner MF, Belew RK, Goodsell DS, et al. AutoDock4 and AutoDockTools4: Automated docking with selective receptor flexibility. J Comput Chem. 2009;30(16):2785-91.

33. Trott O, Olson AJ. AutoDock Vina: ix1mproving the speed and accuracy of docking with a new scoring function, efficient optimization, and multithreading. J Comput Chem. 2010;31(2):455-61.

34. Cai X, Bao L, Dai X, Ding Y, Zhang Z, Li Y. Quercetin protects RAW264.7 macrophages from glucosamine-induced apoptosis and lipid accumulation via the endoplasmic reticulum stress pathway. Mol Med Rep. 2015;12(5):7545-53.

35. Pisonero-Vaquero S, Martínez-Ferreras Á, García-Mediavilla MV, Martínez-Flórez S, Fernández A, Benet M, et al. Quercetin ameliorates dysregulation of lipid metabolism genes via the PI3K/AKT pathway in a diet-induced mouse model of nonalcoholic fatty liver disease. Mol Nutr Food Res. 2015;59(5):879-93.

36. Peleli M, Carlstrom M. Adenosine signaling in diabetes mellitus and associated cardiovascular and renal complications. Mol Aspects Med. 2017;55:62-74.

37. Yu C, Wang Z, Han Y, Liu Y, Wang WE, Chen C, et al. Dopamine D4 receptors inhibit proliferation and migration of vascular smooth muscle cells induced by insulin via down-regulation of insulin receptor expression. Cardiovasc Diabetol. 2014;13:97.

38. Navarro-González JF, Mora-Fernández C. The role of inflammatory cytokines in diabetic nephropathy. J Am Soc Nephrol. 2008;19(3):433-42.

39. Feigerlová E, Battaglia-Hsu SF. IL-6 signaling in diabetic nephropathy: From pathophysiology to therapeutic perspectives. Cytokine Growth Factor Rev. 2017;37:57-65.

40. Lipiec K, Adamczyk P, Świętochowska E, Ziora K, Szczepańska M. L-FABP and IL-6 as markers of chronic kidney damage in children after hemolytic uremic syndrome. Adv Clin Exp Med. 2018;27(7):955-62.

41. Hong JN, Li WW, Wang LL, Guo H, Jiang Y, Gao YJ, et al. Jiangtang decoction ameliorate diabetic nephropathy through the regulation of PI3K/Akt-mediated NF-κB pathways in KK-Ay mice. Chin Med. 2017;12:13.

42. Hu Y, Wang SX, Wu FY, Wu KJ, Shi RP, Qin LH, et al. Effects and mechanism of Ganoderma lucidum polysaccharides in the treatment of diabetic nephropathy in streptozotocin-induced diabetic rats. Biomed Res Int. 2022;2022:4314415.

43. Zhao, T., Lv, J., Zhao, J, Nzekebaloudou M. Hypoxia-inducible factor-1α gene polymorphisms and cancer risk: a meta-analysis. J Exp Clin Cancer Res. 2009;28(1):159.

44. Jin D, Liu F, Yu M, Zhao Y, Yan G, Xue J, et al. Jiedu Tongluo Baoshen formula enhances podocyte autophagy and reduces proteinuria in diabetic kidney disease by inhibiting PI3K/Akt/mTOR signaling pathway. J Ethnopharmacol. 2022;293:115246.

45. Liu F, Fu Y, Wei C, Chen Y, Ma S, Xu W. The expression of GPR109A, NF-kB and IL-1β in peripheral blood leukocytes from patients with type 2 diabetes. Ann Clin Lab Sci. 2014;44(4):443-8.